







## Synthesis and Characterization of Calcium Oxide Nanoparticles (CaO NPS) from Snail Shells Using Hydrothermal Method

Wisdom Chukwuemeke Ulakpa<sup>1\*</sup> , Ijara Maryjane Adaeze<sup>2</sup>, Ohiri Augustine Chimezie<sup>3</sup>, Ayodeji Arnold Olaseinde<sup>4</sup>, Eyide Odeworitse<sup>5</sup>, Erhinyodavwe Onoriode<sup>6</sup>, Oluwatosin Azeez Sarafa<sup>7</sup> , Moses Aderemi Olutoye<sup>7</sup> , Paul Dim<sup>7</sup>, Mohammad Siddique<sup>8</sup> 

<sup>1</sup>Department of Chemical Engineering, Delta State University of Science and Technology, Ozoro, 334111, Nigeria.

<sup>2</sup>Department of Environment, Delta State Ministry of Environment, Asaba, 320109, Nigeria.

<sup>3</sup>Department of Health, Health and Safety Environment, Promasidor Nigeria Limited, Lagos, 100271, Nigeria.

<sup>4</sup>Department of Materials Science and Engineering, College of Engineering, Computing and Applied Sciences, Clemson University, South Carolina, 29631, USA.

<sup>5</sup>Department of Chemical Engineering, University of Delta, Agbor, 321105, Nigeria.

<sup>6</sup>Department of Mechanical Engineering, University of Delta, Agbor, 321105, Nigeria.

<sup>7</sup>Department of Chemical Engineering, Federal University of Technology, Minna, 920211, Nigeria.

<sup>8</sup>Department of Chemical Engineering BUITEMS, Quetta, 87300, Pakistan.

**Abstract:** Calcium oxide (CaO) holds significant importance as a catalyst and effective chemisorbent for hazardous gases. This study presents the synthesis of CaO nanoparticles (NPs) using the hydrothermal technique with snail shells' calcium carbonate (CaCO<sub>3</sub>) as the starting material. The hydrothermal method offers several advantages over alternative approaches for producing metal oxide NPs, including its simplicity, cost-effectiveness, and ability to operate at low temperatures and pressures. By utilizing waste materials like snail shells as a precursor, the entire process becomes more economical, environmentally friendly, and sustainable. The synthesized NPs were analyzed using various techniques, including Fourier transform infrared spectroscopy (FTIR), X-ray powder diffraction (XRD), scanning electron microscope (SEM), transmission electron microscope (TEM), the Barrett-Joyner-Halenda (BJH) model for pore structure quantification, Brunauer-Emmett-Teller (BET) for surface area calculation, and thermo gravimetric analysis (TGA/DTA-DSC). XRD analysis confirmed that the size of the synthesized CaO NPs was 43.14 nm, determined using the Debye-Scherrer equation. The transmission electron microscopy (TEM) image provided valuable insight into the morphology of the nano-catalyst. The analysis revealed that the nano-catalyst displayed a spherical shape, with an average particle size measuring 50 nanometers. The FTIR and XRD results unequivocally demonstrated the successful conversion of calcium carbonate (CaCO<sub>3</sub>) derived from snail shells into calcium oxide (CaO). TGA exhibited a significant weight loss peak at 700 °C, indicating the transformation of CaCO<sub>3</sub> into CaO. The DTA-DSC curve exhibited sharp endothermic peaks at 700 °C, suggesting a decomposition reaction and the formation of a new compound. SEM images displayed porous, rough, and fragile surfaces that became agglomerated at higher temperatures. In other words, the FE-SEM images of NPs illustrated that the particles were predominantly spherical in morphology. Hence, waste snail shells hold promise as a valuable source of calcium for various applications in different fields.

**Keywords:** Calcium oxide NPs, hydrothermal, snailshell, X-ray diffraction, Transmission electron microscope, Brunauer-Emmett-Teller.

**Submitted:** January 8, 2024. **Accepted:** March 20, 2024.

**Cite this:** Chukwuemeke Ulakpa W, Maryjane Adaeze I, Augustine Chimezie O, Arnold Olaseinde A, Odeworitse E, Onoriode E, Azeez Sarafa O, Aderemi Olutoye M, Dim P, Siddique M. Synthesis and Characterization of Calcium Oxide Nanoparticles (CaO NPS) from Snail Shells Using Hydrothermal Method. JOTCSA. 2024;11(2):825-34.

**DOI:** <https://doi.org/10.18596/jotcsa.1416214>

**\*Corresponding author's E-mail:** [ulakpa.wisdom@yahoo.com](mailto:ulakpa.wisdom@yahoo.com)

## 1. INTRODUCTION

The escalating volume of solid waste presents a significant obstacle to establishing a sustainable world. Inadequate waste management practices lead to issues concerning public health and the environment (1). A substantial quantity of solid waste, encompassing municipal, industrial, and hazardous waste, is generated globally. Among these waste products are snail shells, which contribute to environmental degradation and originate from households and restaurants. Snail shells predominantly consist of natural calcium carbonate with limited permeability (1). However, these unwanted materials can be changed to high-quality by-products. Snail shells can serve as a spring of calcium carbonate ( $\text{CaCO}_3$ ) for various applications (2). Unfortunately, the prevailing method of managing waste snail shells involves landfilling, which gives rise to environmental problems. The biodegradation process in landfills, including those that handle food waste, often results in the emission of unpleasant odors. Additionally, the presence of membranes in landfills attracts worms and insects. However, utilizing snail shells can offer several benefits, not only in terms of addressing environmental concerns but also by helping to free up valuable landfill space. The development of nanoparticles has garnered increased awareness due to their superior effectiveness in enhanced surface area. Indeed, scientists have confirmed that nanotechnology has brought about a significant revolution in the field of science. The application of nanotechnology at the nanoscale has indeed unlocked new possibilities and advancements across various scientific disciplines. This progress can be primarily attributed to the unique properties exhibited by nanoparticles (NPs). These properties include an increased surface-to-volume ratio, particle size, charge, shape, and magnetic properties, which differ from their bulk counterparts. Such distinct characteristics of nanoparticles have paved the way for innovative research and applications in fields such as medicine, electronics, materials science, and more, where NPs demonstrate enhanced chemical effectiveness and feasibility at lower temperatures (3). The realm of nanotechnology has made significant strides (4), with NPs finding applications in optical and catalytic domains (3).

In general, materials that have at least one geometrical dimension ranging from 1- 100 nm are typically categorized as nanomaterials (5). Nanocatalysts play a crucial role in various industries because their characteristics are enhanced when they exist in nanosized form. This enhancement is attributed to the larger surface-to-volume ratio of smaller catalysts. Increased pore size and the presence of a vast surface area in nanocatalysts result in a higher number of active sites. As a result, this leads to enhanced catalytic activity and selectivity, along with a longer lifespan and a reduced amount of energy needed to initiate chemical

reactions (6). Furthermore, the utilization of nanocatalysts enables the execution of processes under mild reaction conditions (7).

Calcium oxide is a type of oxide belonging to the group of alkali-earth metals that holds significant potential in various applications. One of its notable advantages is its easy and cost-effective production as nanoparticles (NPs) (4). Calcium oxide nanoparticles ( $\text{CaO}$  NPs) have been effectively employed as catalysts in numerous reactions (3). Additionally, calcium oxide ( $\text{CaO}$ ) finds applications as a pellet for  $\text{CO}_2$  capture and kinetic analysis, as a remediation agent for toxic waste, as an additive in refractory and paint industries, as an antimicrobial agent, as a facilitator for drug delivery, and finding applications in diverse biomedical fields. (8). Its excellent speed and impressive ability to trap carbon dioxide, coupled with its cost-effectiveness and efficiency even in situations with low  $\text{CO}_2$  levels, make it a highly promising candidate for carbon capture (9). Furthermore, it can be utilized for the desulfurization of flue gas and as an emission control to combat pollution, as well as for the purification of hot gases. However, it is important to note that  $\text{CaO}$  is susceptible to air instability and gradually reverts to  $\text{CaCO}_3$  when cooled to room temperature (8).

The synthesis procedures for calcium oxide nanoparticles (NPs) vary, and the process that yields the optimum performance in terms of surface area is always preferred (1). There exist numerous techniques for the production of  $\text{CaO}$  nanoparticles, encompassing sol-gel, thermal decomposition, hydrothermal technique, combustion method, co-precipitation technique, biogenic method, precipitation method, two-step thermal decomposition technique, one-step multi-component synthesis, and microwave synthesis (8). These methods offer the opportunity to customize the physical and chemical properties of nano- $\text{CaO}$ , such as its morphology, specific surface area, and capturing efficiency, under specific synthesis conditions (8). However, most of these methods have limitations such as the use of organic solvents (10), high temperatures, lengthy processing times, and complex equipment (10). Typically,  $\text{CaO}$  nanoparticles are produced by thermally treating precursors like  $\text{Ca}(\text{OH})_2$  or  $\text{CaCO}_3$  (10). In the synthesis of catalysts through thermal hydration-dehydration, three factors significantly impact the catalytic performance of  $\text{CaO}$  catalyst: hydration duration, recalcination temperature, and recalcination duration. The basicity of the  $\text{CaO}$  catalyst, which is directly related to the length of its hydration process (11), can be utilized to estimate its catalytic performance. The objective of this research is to develop calcium oxide ( $\text{CaO}$ ) nanoparticles with high surface area and small particle size using snail shell as a precursor through the hydrothermal method (calcination-hydration-dehydration), to obtain a highly active heterogeneous nanocatalyst. The synthesized particles were characterized using scanning electron microscopy (SEM), X-ray diffraction (XRD), and

Chukwuemeke Ulakpa W et al. JOTCSA. 2024; 11(2): 825-834  
transmission electron microscopy (TEM), as well as BET (Brunauer-Emmett-Teller) and thermogravimetric-differential scanning calorimetry (TG-DSC) techniques to determine their suitability for industrial applications.

## 2. EXPERIMENTAL SECTION

### 2.1. Materials and Methods

The snail shells were obtained from a nearby restaurant and market, specifically from a dealer who specializes in snail shells. For the experiments, deionized water (H<sub>2</sub>O) was utilized with a remarkable purity level of 99%. Furthermore, all the chemicals employed in the experiments were of analytical grade.

### 2.2. Synthesis of Calcium Oxide Nanoparticles (CaO NPs)

The synthesis of calcium oxide nanoparticles (CaO NPs) involved the preparation of a highly active CaO catalyst through a series of steps including calcination, hydration, and dehydration using snail shells. To begin, the snail shells were thoroughly washed to remove any unwanted materials adhering to their surface. They were then rinsed with distilled water. The washed shells were dried in a hot air oven at a temperature of 110°C for a duration of 12 hours. After drying, the shells were crushed into smaller pieces using a blender, ensuring they could pass through a 60µm sieve. Subsequently, the crushed shells were calcined in a muffle furnace under static air conditions at a temperature of 900°C for a period of 3 hours. This process aimed to transform the calcium species within the shells into CaO particles.

The CaO derived from the shells was then subjected to refluxing in water at a temperature of 80°C. The mixture was stirred for 2 hours using a magnetic stirrer set at 350 rpm and allowed to settle for 12 hours. The resulting whitish product was ground, filtered, and subsequently dried in a hot air oven overnight at a temperature of 120°C. To convert the hydroxide form of the product into its oxide form, the solid product underwent dehydration through recalcination at a temperature of 700°C for a duration of 3 hours. This process yielded a finely powdered white catalyst of nano CaO. To ensure the stability of the obtained product, it was stored in a desiccator to prevent reactions with carbon dioxide and humidity in the air before use. Finally, the samples were subjected to characterization to analyze their properties.

### 2.3. Characterization of The Synthesized Nanoparticles (NPs)

For this study, several scientific techniques were employed. Fourier-transform infrared spectroscopy (FTIR), thermogravimetric analysis (TGA-DTG-DSC), X-ray diffraction (XRD), Brunauer-Emmett-Teller

## RESEARCH ARTICLE

(BET/BJH), scanning electron microscope (SEM), and transmission electron microscope (TEM) were utilized. To conduct crystal structural analysis, X-ray diffraction (XRD) was employed. The diffraction angles (2θ) used ranged from 10 to 90 degrees. Cu Kα radiation (λ = 1.5406 Å) was used as the source of radiation for this analysis. To examine the size, shape, and surface morphology of the nanoparticle, a field emission scanning electron microscope (FE-SEM) with a coater (Quorum Q150T ES/10 mA, 120 s Pt coating) was used. The accelerating voltage for this microscope was set at 10 kV. To determine the different functional groups present in the synthesized nanoparticle, FTIR spectroscopy (FT-IR) (6700 FTIR) was employed. The specific surface area, pore size, and pore volume of the nanocatalyst were measured using N<sub>2</sub> adsorption/desorption isotherm. This analysis was performed using a BET surface area analyzer (Micromeritics ASAP 2020V1.05 software). Powder X-ray diffraction (XRD) was carried out using a Rigaku MiniFlex-300/600 to determine the catalytic phases. The diffractogram was developed within a 2θ range of 10°-80° with a scan rate of 10°/min. The obtained XRD data was compared with the database of the 'Joint Committee on Powder Diffraction Standards' (JCPDS) to confirm the exact catalyst phase. Finally, the chemical analysis of the synthesized CaO nanoparticle was performed using an X-ray fluorescence spectrometer (Shimadzu, Japan).

## 3. RESULTS AND DISCUSSION

### 3.1. Fourier Transform Infrared Analysis (FTIR) of CaONPs

Figure 1 illustrates the results of the Fourier Transform Infrared (FTIR) analysis conducted on calcium oxide (CaO) nanoparticles. The spectra revealed several absorption bands at specific wavenumbers: 3716.2, 2512.2, 2113.4, 1982.9, 1897.2, 1796.6, 1394.0, 872.2, 711.9, and 663.5 cm<sup>-1</sup>. The sharp absorption band observed at 2512.2 cm<sup>-1</sup> can be attributed to the stretching vibrations of hydroxyl (O-H) groups. This band is a result of the formation of calcium hydroxide (Ca(OH)<sub>2</sub>) through the hydration process of CaO (12). Furthermore, the broad peak at 2113.4 cm<sup>-1</sup> indicates the presence of physically adsorbed water molecules attached to the nanoparticles, as it signifies the -OH stretching vibrations (13). Additionally, absorption bands at 1982.9 and 1796.6 cm<sup>-1</sup> correspond to the absorption of CO<sub>2</sub> on the nanoparticle's surface and the stretching vibrations of the Ca-OH bonds, respectively (14). The most prominent peaks observed at 1394.0, 872.2, and 711.9 cm<sup>-1</sup> confirm the presence of calcium oxide nanoparticles, as they are assigned to the vibrations of the Ca-O bonds (12, 14).

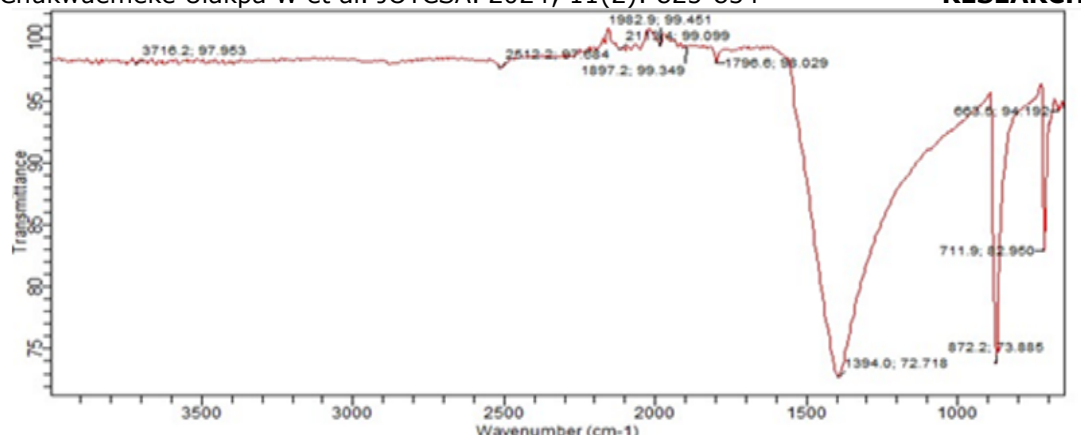


**Figure 1:** Fourier Transform Infrared analysis (FTIR) of CaONPs.

### 3.2. X-ray Fluorescence (XRF) Analysis

The chemical makeup of the CaO NPs in this investigation can be found in Table 1. The primary constituents of the catalyst include oxygen (O), calcium (Ca), aluminum (Al), titanium (Ti), and magnesium (Mg). Additionally, it comprises various metallic oxides, namely silicon dioxide (SiO<sub>2</sub>), vanadium pentoxide (V<sub>2</sub>O<sub>5</sub>), chromium trioxide (Cr<sub>2</sub>O<sub>3</sub>), manganese oxide (MnO), iron oxide (Fe<sub>2</sub>O<sub>3</sub>), cobalt oxide (Co<sub>3</sub>O<sub>4</sub>), nickel oxide (NiO), copper

oxide (CuO), niobium oxide (Nb<sub>2</sub>O<sub>3</sub>), tungsten trioxide (WO<sub>3</sub>), diphosphorus pentoxide (P<sub>2</sub>O<sub>5</sub>), sulfur trioxide (SO<sub>3</sub>), calcium oxide (CaO), magnesium oxide (MgO), potassium oxide (K<sub>2</sub>O), barium oxide (BaO), aluminum oxide (Al<sub>2</sub>O<sub>3</sub>), tantalum pentoxide (Ta<sub>2</sub>O<sub>5</sub>), titanium dioxide (TiO<sub>2</sub>), zinc oxide (ZnO), silver oxide (Ag<sub>2</sub>O), chlorine (Cl), zirconium dioxide (ZrO<sub>2</sub>), and tin dioxide (SnO<sub>2</sub>). These components are also believed to serve as the primary active sites of the catalyst (15).

**Table 1:** X-ray fluorescence (XRF) of synthesized CaONPs.

Elements	Weight/Concentration (wt%)		
O	29.113	Fe	0.072
Mg	0.000	Co	0.051
Al	1.872	Ni	0.028
Si	0.087	Cu	0.044
P	0.000	Zn	0.006
S	0.091	Zr	0.073
Cl	0.256	Nb	0.291
K	0.057	Ag	0.000
Ca	67.178	Sn	0.571
Ti	0.021	Ba	0.052
V	0.013	Ta	0.063
Cr	0.001	W	0.046
Mn	0.014	Total	100.00

### 3.3. Brunauer-Emmett-Teller-BET-(Textural Properties Analysis)/Barrett-Joyner-Halenda (BJH) Method

The results obtained from the BET and BJH analyses of the artificially produced nano-CaO revealed that it had a surface area of 5.11 square meters per gram, an average pore diameter of 1.1 nanometers, and a pore volume of 0.002556 cubic centimeters per gram. On the other hand, the reported average pore diameter of the nanoparticles (NPs) ranged from greater than 2 nanometers to 50 nanometers, indicating the presence of both microspores and active sites on the external surface of the nano-CaO catalyst. It is worth noting that the total surface area

often plays a crucial role in determining the catalytic performance of a catalyst. Therefore, in this study, we measured the surface areas of the synthesized catalysts to understand the impact of the total surface area on the catalytic reaction. Figure 2 displays the BET plot of the synthesized CaO NPs, while Figures 3(a) and 3(b) represent the nitrogen adsorption-desorption isotherms and pore distribution of the synthesized CaO NPs, respectively. The NPs exhibited a characteristic type III isotherm with a hysteresis loop of H3 type, indicative of a micro-porous structure. This implies that the prepared NPs possess a micro-porous structure, which further supports the presence of microspores on the catalyst's surface.

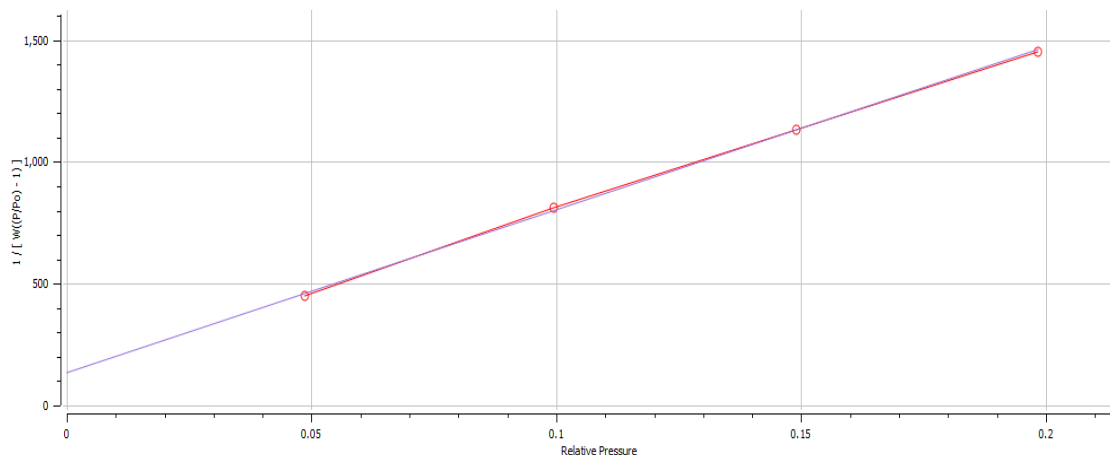


Figure 2: BET plot of CaO NPs.

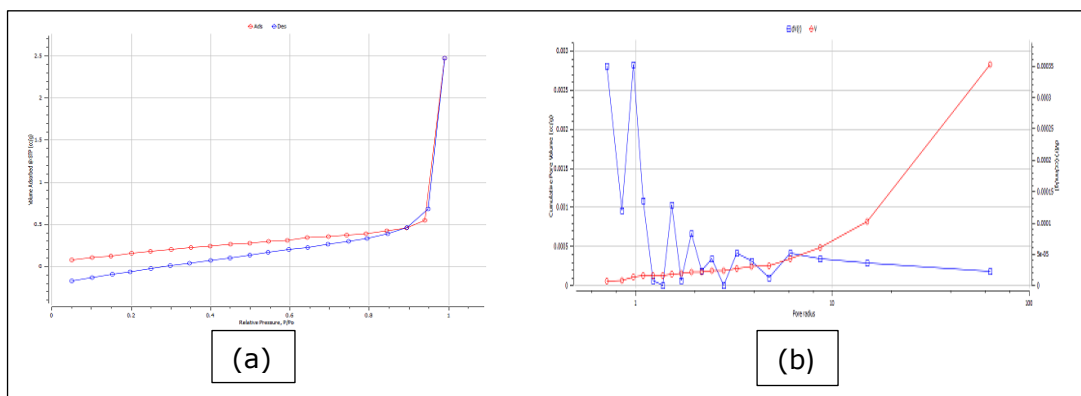
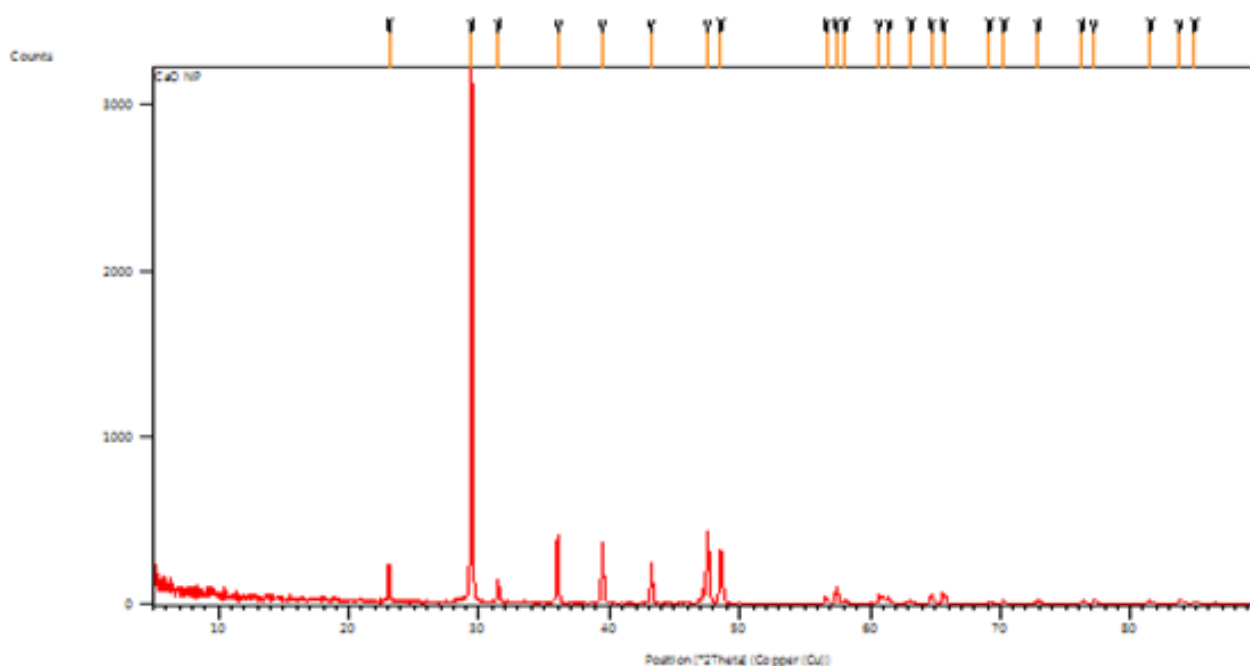


Figure 3: (a): N<sub>2</sub> adsorption-desorption isotherm of CaO NPs, (b): Barrett-Joyner-Halenda (BJH) pore size and pore volume distribution (desorption isotherm) of CaO NPs.

**3.4. X-ray Diffraction (XRD) Analysis**

X-ray diffraction analysis (XRD) was employed for the characterization of the catalysts (16). As the samples were in the form of polycrystalline powder, the XRD analysis focused on identifying specific lattice planes that generated peaks at corresponding angular positions, known as 2θ, as determined by Bragg's law (16). The 2θ peaks observed for CaO nanoparticles were found at angles of 23.09°, 29.44°, 31.45°, 36.06°, 39.44°, 43.19°, 47.53°, 48.53°, 56.20°, 57.41°, 58.12°, 60.67°, 61.44°, 63.16°, 64.70°, 65.64°, 69.16°, 70.28°, 72.92°, 76.29°, 77.16°, 81.53°, 83.75°, and 84.90°. These peaks displayed a significant resemblance to the standard ICDD (The International Centre for Diffraction Data) file for CaO (JCPDS: 00-005-0586), with corresponding values of (h k l) as (0 1 2), (1 0 4), (0 0 6), (1 1 0), (1 1 3), (2 0 2), (0 1 8), (1 1 6), (2 1 1), (1 2 2), (1 0 1), (2 1 4), (1 1 9), (1 2 5), (3 0 0), (0 0 1), (2 1 7), (0 2 1), (1 2 8), (2 2 0), (1 1

1), (2 1 1), (1 3 4), and (2 2 6), respectively. These planes corresponded to the calcite phase and were observed in the nano CaO catalyst prepared through thermal-hydration-dehydration treatment. The XRD pattern confirmed the formation of calcium oxide in the cubic phase (17, 18), which aligned with the findings of previous studies (19, 20). The average crystallite sizes (D) were determined using the full width at half maximum (FWHM) of the XRD peaks, following Debye-Scherrer's equation:  $D = K\lambda/(\beta \cos\theta)$ , where β represents the full width at half maximum (FWHM) in radians and θ is the position of the maximum diffraction peak (incident angle of the X-ray). The shape factor, K, typically around 0.9, was also considered. In this study, the X-ray wavelength (λ) used was 1.5406 Å for Cu Kα. Applying Debye-Scherrer's equation, the average crystallite size of the CaO nanoparticles was calculated to be 43.14 nm, while the particle size of the synthesized nanoparticles ranged from 20.07 to 70.25 nm.



**Figure 4:** XRD pattern of synthesized CaO NPs.

**Table 2:** Peak angles and their corresponding (h k l) planes, peak height, full width at half maximum, d-spacing, relative intensity, and crystallite sizes of CaO NPs.

Peak number	Peak Pos.( $2\theta^\circ$ )	Miller indices (h k l)	Peak-Height (cts)	FWHM ( $2\theta^\circ$ )	d-spacing ( $\text{\AA}$ )	Rel. Int. (%)	D *. nm	Average D (nm)
1	23.0923	(0 1 2)	223.73	0.1476	3.85166	6.97	56.10	43.14
2	29.4474	(1 0 4)	3209.89	0.1476	3.03329	100.00	56.10	
3	31.4552	(0 0 6)	137.26	0.1476	2.84411	4.28	56.16	
4	36.0610	(1 1 0)	387.89	0.1771	2.49073	12.08	46.92	
5	39.4463	(1 1 3)	366.73	0.1771	2.28442	11.42	46.92	
6	43.1931	(2 0 2)	239.36	0.2066	2.09455	7.46	41.16	
7	47.5289	(0 1 8)	416.78	0.1476	1.91310	12.98	56.23	
8	48.5328	(1 1 6)	322.68	0.1476	1.87585	10.05	56.10	
9	56.6280	(2 1 1)	32.08	0.1771	1.62541	1.00	46.86	
10	57.4113	(1 2 2)	80.52	0.1771	1.60508	2.51	46.84	
11	58.1288	(1 0 1)	19.56	0.2362	1.58697	0.61	35.13	
12	60.6790	(2 1 4)	57.46	0.1181	1.52624	1.79	70.25	
13	61.4462	(1 1 9)	32.39	0.1771	1.50901	1.01	46.87	
14	63.1679	(1 2 5)	13.66	0.3542	1.47196	0.43	23.41	
15	64.7045	(3 0 0)	56.14	0.1181	1.44067	1.75	70.25	
16	65.6424	(0 0 1)	63.44	0.1476	1.42234	1.98	56.21	
17	69.1648	(2 1 7)	9.16	0.3542	1.35826	0.29	23.42	
18	70.2817	(0 2 1)	19.50	0.3542	1.33939	0.61	23.42	
19	72.9271	(1 2 8)	22.30	0.3542	1.29719	0.69	23.42	
20	76.2934	(2 2 0)	10.16	0.2362	1.24812	0.32	35.12	
21	77.1636	(1 1 1)	21.77	0.4133	1.23621	0.68	20.07	
22	81.5328	(2 1 1)	18.18	0.1771	1.18065	0.57	46.87	
23	83.7588	(1 3 4)	20.64	0.2952	1.15485	0.64	28.10	
24	84.9228	(2 2 6)	8.15	0.3542	1.14197	0.25	23.42	

\* D: The crystallite size (nm)

### 3.5. Scanning Electron Microscopy (SEM) Analysis

The image displayed in Figure 5 illustrates the physical appearance of the CaO nanoparticles that were synthesized. The scanning electron microscopy (SEM) image reveals that the particles have an irregular shape with a rough surface and fractured texture. Additionally, the particles tend to have a

spherical shape and possess a porous structure with numerous cavities, similar to a porous material. This porous structure is believed to contribute to the increased presence of basic sites on the catalyst, as mentioned in reference (21). The porosity observed in the CaO nanoparticles is attributed to the release of a significant amount of gaseous water molecules



during the decomposition of  $\text{CaCO}_3 \cdot \text{H}_2\text{O}$ , as reported in reference (12).

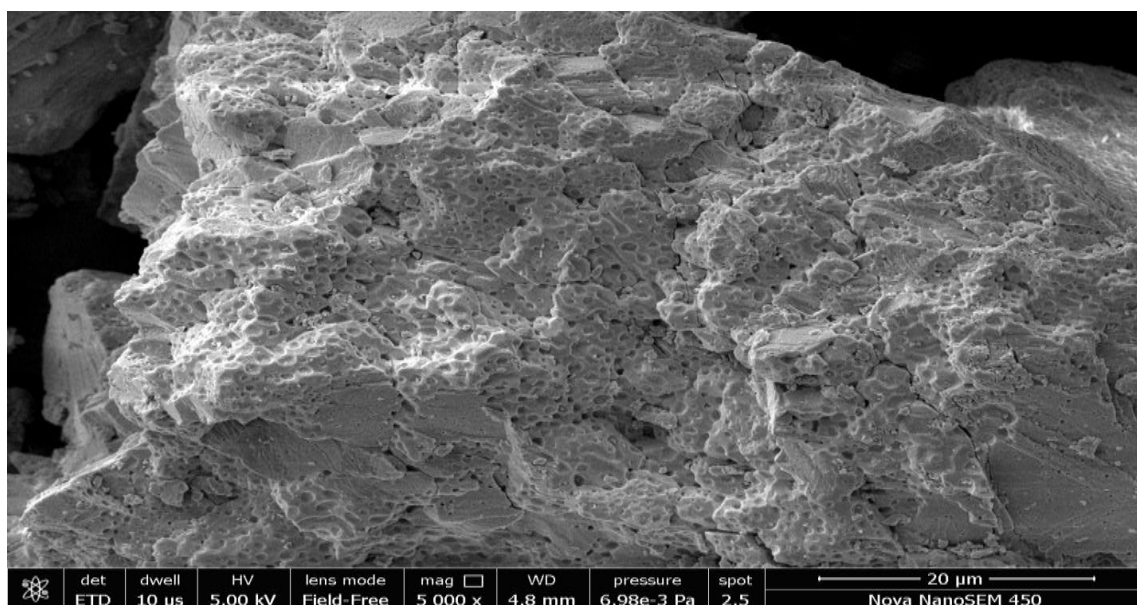


**Figure 5:** Scanning electron microscope of synthesized CaO NPs.

### 3.6. High-Resolution Transmission Electron Microscopy (HRTEM)

The high-resolution transmission electron microscope (HR-TEM) is a valuable technique for determining the characteristics of particles, such as their morphology, phase, and structural properties. It also provides crystallographic information. Additionally, HR-TEM is useful for identifying the mesoporous structure of nanoparticles. Figure 6 illustrates the HRTEM image of CaO nanoparticles.

Upon analyzing the high-resolution TEM micrograph (Figure 6), it was discovered that the CaO

nanoparticles exhibited a particulate morphology, with particle sizes smaller than 50 nm. Notably, the nano-CaO particles tended to agglomerate, forming larger and spherical particles, as depicted in Figure 6. The particle size observed using TEM corresponds well with the average crystallite size estimated by X-ray diffraction (XRD). This finding aligns with the results reported by (22).

Furthermore, the presence of crystallites contributes to an increase in the surface area, thereby enhancing the interaction between reactants and the catalyst surface.

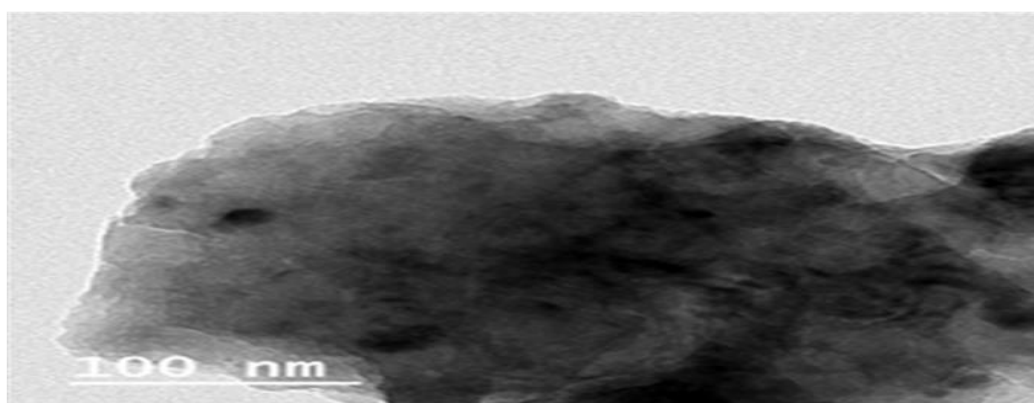


**Figure 6:** HRTEM image of CaO NPs.

### 3.7. Thermogravimetric Analysis (TGA)/Differential Thermal Analysis (DTA/DSC)

The synthesized calcium oxide nanoparticles (CaO NPs) were subjected to thermal gravimetric analysis (TGA) and differential thermal analysis (DTA)/differential scanning calorimetry (DSC) to comprehend the influence of elevated temperatures on their thermal ability to withstand heat, as well as to identify the thermal transitions occurring during

the process. Figure 7 presents the TGA/DTA-DSC curve of the CaO NPs. The TGA curve demonstrates a significant weight loss of the catalyst (approximately 43%) at higher temperatures (700 °C). The weight reduction can be ascribed to the disintegration of carbonic material, resulting in the formation of carbon monoxide (CO) and carbon dioxide ( $\text{CO}_2$ ), as well as the elimination of water from calcium hydroxide ( $\text{Ca}(\text{OH})_2$ ) and the

decomposition of calcium carbonate (CaCO<sub>3</sub>) (12). Furthermore, the DTA/DSC curve supports these findings by revealing sharp endothermic peaks within the temperature range of 700-800 °C. These peaks indicate decomposition reactions and the formation

of new compounds. Therefore, the TGA/DTA-DSC results conclusively confirm that a high temperature is necessary for the calcination process of CaO nanoparticles.

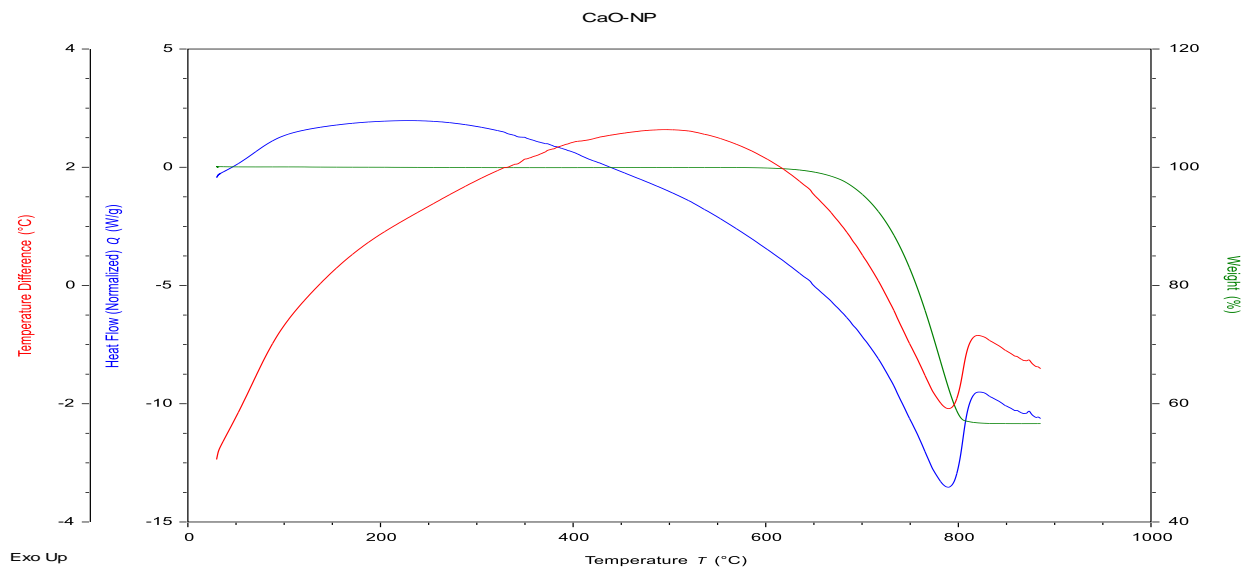


Figure 7: TGA/DTA-DSC of CaO NPs.

**3.8. X-ray Photoelectron Spectroscopy (XPS) Analysis of CaONPs**

A comprehensive examination using X-ray photoelectron spectroscopy (XPS) was conducted to ascertain the chemical composition and bonding state of the CaO nanoparticle catalysts. The XPS full survey spectrum, displayed in Figure 8, provides insights into the presence of oxygen (O), calcium (Ca), and carbon (C) on the catalyst's surface. By deconvoluting the C 1s spectra, two distinct peaks were observed at 284.36eV and 289.31eV binding

energy, with a full width at half maximum (FWHM) of 2.7eV. These peaks indicate the existence of metal carbonates, specifically C-C and C=O bonds. The O1s spectrum shows a peak at 530.95 eV, suggesting the presence of metal oxide. Furthermore, the deconvoluted Ca2p spectrum exhibits peaks at 346.28 eV and 350.12 eV, indicating the occurrence of calcium oxide (CaO) and calcium carbonate (CaCO<sub>3</sub>), respectively. Detailed information about the XPS survey peaks can be found in Table 3.

Table 3: XPS survey Peaks of CaO NPs.

	Name	Peak Binding Energy (eV)	FWHM eV	Area (P) CPS.eV	Atomic %
CaO NPs	O1s	530.95	2.76	1814758.72	47.19
	C1s	284.36, 289.14	2.7	617465.92	38.83
	Ca2p	346.28, 350.12	2.72	1273838.92	13.97



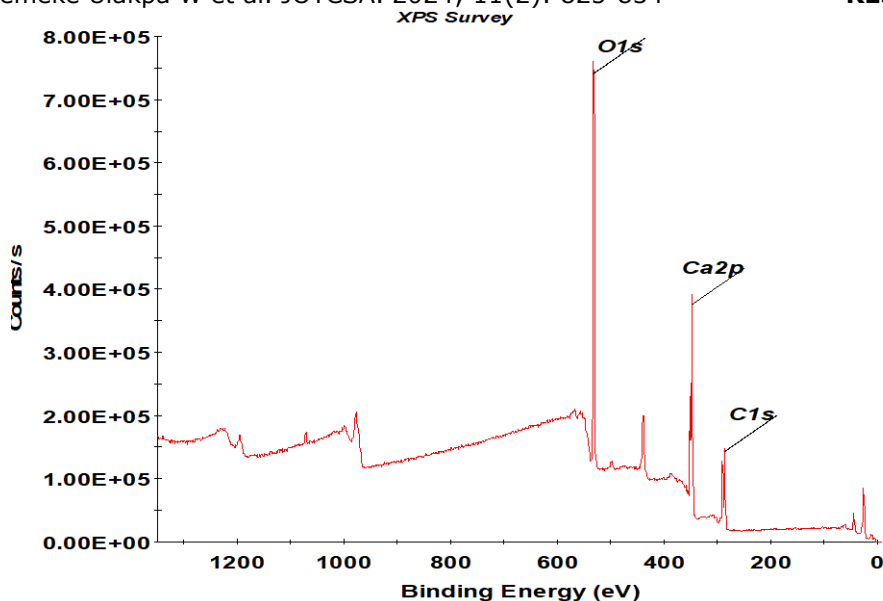


**Figure 8:** XPS full survey spectrum of CaO NPs.

#### 4. CONCLUSION

In conclusion, this research demonstrates that calcium oxide (CaO) nanoparticles can be successfully produced using the hydrothermal method with calcium carbonate ( $\text{CaCO}_3$ ) as a precursor. The process involves heating the  $\text{CaCO}_3$  at a temperature of 900 °C for 3 hours and then recalcining it at 700 °C for another 3 hours. The resulting CaO nanoparticles exhibit a nearly spherical morphology, as observed through scanning electron microscopy (SEM) images.

Furthermore, the BET (Brunauer-Emmett-Teller) analysis reveals that the prepared nanoparticles possess micropore range porosity. This indicates their potential for various applications. X-ray diffraction investigations validate the polycrystalline characteristic of the CaO nanoparticles. The proposed method is both simple and convenient, eliminating the need for organic solvents, expensive raw materials, or complex equipment. As a result, it offers an economical approach to synthesizing calcium oxide particles on a large scale, utilizing snail shells as a sustainable source of calcium carbonate. The findings of this research highlight the promising capabilities of CaO nanoparticles in serving as effective drug carriers, given their bioactive and biocompatible properties. Furthermore, the particle surfaces exhibit micropores with a surface area of 5.11  $\text{m}^2/\text{g}$ , an average pore diameter of 1.1 nm, and a pore volume of 0.00255  $\text{cm}^3/\text{g}$ . These characteristics further enhance the nanoparticles' potential for various applications.

In addition, this research contributes to the conversion of agricultural waste into valuable resources. The hydrothermal treatment of snail shells, combined with the synthesized catalyst, results in the formation of calcium oxide (CaO). This not only provides a sustainable solution for waste management but also presents an opportunity for resource utilization.

In summary, this study demonstrates the successful production of CaO nanoparticles using a hydrothermal method. The nanoparticles exhibit desirable properties, making them suitable for various applications, including drug delivery. Furthermore, the incorporation of snail shells as a primary resource aids in the promotion of sustainable agricultural waste management.

#### 5. CONFLICT OF INTEREST

The authors declare no conflict of interest.

#### 6. ACKNOWLEDGMENTS

The authors are grateful to the Department of Agricultural and Bioresources Engineering, Futminna for their assistance in carrying out the research work in their Laboratory. The authors are also grateful to Scientium analyze solutions, India.

#### 7. REFERENCES

- Habte L, Shiferaw N, Mulatu D, Thenepalli T, Chilakala R, Ahn J. Synthesis of Nano-Calcium Oxide from Waste Eggshell by Sol-Gel Method. *Sustainability* [Internet]. 2019 Jun 7;11(11):3196. Available from: [<URL>](#).
- Cree D, Rutter A. Sustainable Bio-Inspired Limestone Eggshell Powder for Potential Industrialized Applications. *ACS Sustain Chem Eng* [Internet]. 2015 May 4;3(5):941–9. Available from: [<URL>](#).
- Alobaidi YM, Ali MM, Mohammed AM. Synthesis of Calcium Oxide Nanoparticles from Waste Eggshell by Thermal Decomposition and their Applications. *Jordan J Biol Sci* [Internet]. 2022 Jun 1;15(2):269–74. Available from: [<URL>](#).
- Bano S, Pillai S. Green synthesis of calcium oxide nanoparticles at different calcination temperatures. *World J Sci Technol Sustain Dev* [Internet]. 2020 May 19;17(3):283–95. Available from: [<URL>](#).

5. Bensebaa F. Nanoparticle Fundamentals. In: Interface Science and Technology [Internet]. Elsevier; 2013. p. 1–84. Available from: [<URL>](#).
6. Banković–Ilić IB, Miladinović MR, Stamenković OS, Veljković VB. Application of nano CaO–based catalysts in biodiesel synthesis. *Renew Sustain Energy Rev* [Internet]. 2017 May 1;72:746–60. Available from: [<URL>](#).
7. Serp P, Philippot K. Nanomaterials in Catalysis [Internet]. Serp P, Philippot K, editors. *Nanomaterials in Catalysis: First Edition*. Wiley; 2013. Available from: [<URL>](#).
8. Khine EE, Koncz-Horvath D, Kristaly F, Ferenczi T, Karacs G, Baumli P, et al. Synthesis and characterization of calcium oxide nanoparticles for CO<sub>2</sub> capture. *J Nanoparticle Res* [Internet]. 2022 Jul 1;24(7):139. Available from: [<URL>](#).
9. Granados-Pichardo A, Granados-Correa F, Sánchez-Mendieta V, Hernández-Mendoza H. New CaO-based adsorbents prepared by solution combustion and high-energy ball-milling processes for CO<sub>2</sub> adsorption: Textural and structural influences. *Arab J Chem* [Internet]. 2020 Jan 1;13(1):171–83. Available from: [<URL>](#).
10. Mirghiasi Z, Bakhtiari F, Darezereshki E, Esmailzadeh E. Preparation and characterization of CaO nanoparticles from Ca(OH)<sub>2</sub> by direct thermal decomposition method. *J Ind Eng Chem* [Internet]. 2014 Jan 25;20(1):113–7. Available from: [<URL>](#).
11. Asikin-Mijan N, Taufiq-Yap YH, Lee HV. Synthesis of clamshell derived Ca(OH)<sub>2</sub> nano-particles via simple surfactant-hydration treatment. *Chem Eng J* [Internet]. 2015 Feb 15;262:1043–51. Available from: [<URL>](#).
12. Gaurav K, Kumari S, Dutta J. Utilization of Waste Chicken Eggshell as Heterogeneous CaO Nanoparticle for Biodiesel Production. *J Biochem Technol* [Internet]. 2021 Jun 17;12(1):49–57. Available from: [<URL>](#).
13. Sumathi N. Optical characterization of calcium oxide nanoparticles. *Int J Adv Technol Eng Sci*. 2017;5(2):63–7.
14. Kalanakoppal Venkatesh Y, Mahadevaiah R, Haraluru Shankaraiah L, Ramappa S, Sannagoudar Basanagouda A. Preparation of a CaO Nanocatalyst and Its Application for Biodiesel Production Using *Butea monosperma* Oil: An Optimization Study. *J Am Oil Chem Soc* [Internet]. 2018 May 19;95(5):635–49. Available from: [<URL>](#).
15. Rajkumari K, Rokhum L. A sustainable protocol for production of biodiesel by transesterification of soybean oil using banana trunk ash as a heterogeneous catalyst. *Biomass Convers Biorefinery* [Internet]. 2020 Dec 28 [cited 2024 Mar 22];10(4):839–48. Available from: [<URL>](#).
16. Charles Ugbede A, Elizabeth Jumoke E, Abdullahi Abdullahi M. Development and Application of Heterogeneous Catalyst from Snail Shells for Optimization of Biodiesel Production from *Moringa Oleifera* Seed Oil. *Am J Chem Eng* [Internet]. 2021;9(1):1–17. Available from: [<URL>](#).
17. Almutairi FM. Biopolymer Nanoparticles: A Review of Prospects for Application as Carrier for Therapeutics and Diagnostics. *Int J Pharm Res Allied Sci* [Internet]. 2019;8(1):25–35. Available from: [<URL>](#).
18. Babaei H, Sepahy AA, Amini K, Saadatmand S. The effect of titanium dioxide nanoparticles synthesized by bacillus tequilensis on clb gene expression of colorectal cancer-causing Escherichia coli. *Arch Pharm Pract*. 2020;11(1):22–31.
19. Gupta J, Agarwal M. Preparation and characterization of CaO nanoparticle for biodiesel production. *AIP Conf Proc* [Internet]. 2016 Apr 13;1724(1):020066. Available from: [<URL>](#).
20. Bet-Moushoul E, Farhadi K, Mansourpanah Y, Nikbakht AM, Molaei R, Forough M. Application of CaO-based/Au nanoparticles as heterogeneous nanocatalysts in biodiesel production. *Fuel* [Internet]. 2016 Jan 15;164:119–27. Available from: [<URL>](#).
21. Simpen IN, Winaya INS, Subagia IDGA, Suyasa IWB. Green Nano-Composite of CaO/K-Sulfated TiO<sub>2</sub> and Its Potential as a Single-Step Reaction Solid Catalyst for Biofuel Production. *KnE Life Sci* [Internet]. 2022 Jun 7;2022:382-392–382–392. Available from: [<URL>](#).
22. Kodeh FS, El-Nahhal IM, Elkhair EA, Darwish AH. Synthesis of CaO–Ag-NPs @CaCO<sub>3</sub> Nanocomposite via Impregnation of Aqueous Sol Ag-NPs onto Calcined Calcium Oxalate. *Chem Africa* [Internet]. 2020 Sep 14;3(3):679–86. Available from: [<URL>](#).